Preparation and Characterization of Composites of Polyethylene with Polypyrrole-Coated Wollastonite

Chu Kuen Ong, Sudip Ray, Ralph P. Cooney, Neil R. Edmonds, Allan J. Easteal

Department of Chemistry and Centre for Advanced Composite Materials, The University of Auckland, Private Bag 92019, Auckland, New Zealand

Received 24 September 2007; accepted 11 May 2008
DOI 10.1002/app.28698
Published online 9 July 2008 in Wiley InterScience (www.interscience.wiley.com).

ABSTRACT: Composite sheets of polyethylene and polypyrrole-coated wollastonite were prepared by extrusion and compression molding. Four compatibilizers were also evaluated, poly(ethylene-*co*-methyl acrylate) (EMA), maleated polyethylene (MAPE), poly(ethylene-*co*-vinyl alcohol) (EVOH), and poly(vinyl alcohol) (PVOH). The composite materials were characterized using X-ray diffraction, thermogravimetric analysis, scanning electron microscopy (SEM), Raman spectroscopy, and mechanical properties determined by tensile tests. SEM micrographs showed that significantly improved interactions occurred between the PE matrix and polypyrrole-coated wollastonite particles in the presence of EMA, MAPE, and EVOH. Raman spectroscopy confirmed that the polypyrrole coating on the wollastonite particles was not thermally degraded during melt processing. © 2008 Wiley Periodicals, Inc. J Appl Polym Sci 110: 632–640, 2008

Key words: composites; conducting polymer; mechanical properties; polyethylene; polypyrrole

INTRODUCTION

Conducting polymers have potential applications in electronics circuitry, electromagnetic shielding, conductive coatings, as antioxidants and in many other fields. Although they are brittle, infusible materials, and difficult to process due to their aromatic nature, interchain hydrogen bonding, and charge delocalization,[1] their desirable physical and mechanical properties can be captured in composites made by blending conducting polymers with commodity thermoplastics using thermal processing techniques.[2,3]

Polypyrrole is one of the most attractive conducting polymers because of its ease of synthesis and useful properties. It has relatively high conductivity, good environmental stability under ambient conditions, and low toxicity.[4] Polypyrrole has been coated onto a variety of substrates, including inorganic minerals (wollastonite, clay, talc, and mica),[5] conventional organic polymer powders such as polyethylene (PE), polypropylene, poly(vinyl chloride),[6] and ordered mesoporous siliceous materials such as MCM-41 and SBA-15, and on Canadian-dried switch-milled grass to obtain a composite with good mechanical and antistatic properties.[7]

Correspondence to: A. J. Easteal (aj.easteal@auckland.ac.nz).
Contract grant sponsor: Foundation for Research, Science and Technology, New Zealand; contract grant number: UOAX0408.

© 2008 Wiley Periodicals, Inc.

Wollastonite is a naturally occurring form of calcium silicate with acicular crystal habit. It is commonly used in the ceramic and cement industries[8] and has been reported to act as a reinforcing material in rotational-molded PE.[9] More recently, the growth of the bioactive material hydroxycarbonate apatite on the surface of a plasma-sprayed wollastonite coating soaked in simulated body fluid has shown wollastonite to be an excellent potential candidate for biomaterials applications,[8] especially in orthopaedics.[10]

The goal of this study was to incorporate polypyrrole-coated wollastonite in PE using a screw extruder and to evaluate the efficacy of compatibilizers in enhancing the interaction between the polypyrrole coating and the PE matrix. Four potential compatibilizers were used, poly(ethylene-*co*-methyl acrylate) (EMA), maleated polyethylene (MAPE), poly(ethylene-*co*-vinyl alcohol) (EVOH), and poly(vinyl alcohol) (PVOH).

EXPERIMENTAL

Materials

Pyrrole (Acros Organics) was distilled at reduced pressure and stored in the dark under nitrogen at 4°C before use. Ammonium persulphate (BDH Chemicals), wollastonite (from Wolkem's Mines, India), EMA (Elvaloy 1820, Du Pont), MAPE (Exxelor VA 1840, ExxonMobil), EVOH (E105B, Kuraray), polyvinyl alcohol (BP-05, Chang Chun), and linear

medium density PE (Cotene 9042, provided by J. R. Courtenay, Auckland) were used as received.

Synthesis of polypyrrole

One milliliter of pyrrole was added dropwise to 340 mL of 0.1*M* aqueous $(NH_4)_2S_2O_8$ at room temperature whereupon the solution darkened very rapidly as polypyrrole formed. After stirring the reaction mixture for 2 h, the precipitated polypyrrole was filtered and washed with water, then with methanol to remove unreacted pyrrole and oligomers, and vacuum dried at 80°C overnight.

Coating polypyrrole on wollastonite

Wollastonite (5 g) was stirred in 200 mL of water for 15 min to ensure optimal separation into individual particles. Thirty milliliters of 0.45*M* aqueous $(NH_4)_2S_2O_8$ was then added to the suspension, and the mixture was stirred for 10 min. Pyrrole (0.4 mL) was dispersed in 5 mL of water and added dropwise to the wollastonite suspension. The reaction mixture was stirred continuously for about 1 h to form a polypyrrole coating on the wollastonite particles. The product (referred to hereafter as wollastonite-ppy) was filtered and washed with water and methanol to remove unreacted pyrrole and then dried in vacuum at 80°C overnight. This procedure gave a 4.8% increase in mass of the wollastonite after coating.

Thermal processing of PE/wollastonite-ppy composites

Polyethylene (PE) powder was mixed with compatibilizer in the weight ratio (PE : compatibilizer) 9 : 1 and wollastonite-ppy (predried at 80°C in vacuum for 12 h) to give a mixture containing 5 phr wollastonite-ppy relative to PE + compatibilizer. The mixture was then melt blended using an Axxon BX-18 single screw extruder with screw diameter 18 mm and L/D ratio = 30. The temperatures of the heated zones of the extruder from the first heated section to the die were 150, 170, 180, 180, 180, and 180°C, respectively, and the screw rotation speed was 65 rpm. The extrudate was granulated then compression molded with an applied pressure of 1 ton at 180°C for 3 min to make a sheet ~ 300-μm thick.

Characterization

X-ray powder diffraction patterns were obtained using a Bruker D8 Advance X-ray diffractometer with Cu Kα radiation.

Thermogravimetric analysis was carried out on ~ 5 mg samples using a Thorn TGA/STA 1500 instrument at a heating rate of 10°C min^{-1} in an atmosphere of air.

Polypyrrole and wollastonite-ppy powder were pressed into a pellet for conductivity measurement. The conductivity of the polypyrrole pellet was determined at ambient temperature using a Jandal Multi Height four-point probe with a DC current source. Because the wollastonite-ppy pellet and composite sheets had too low conductivity to be measured using the Jandal electrometer, the conductivity was determined using a Keithley 6517A high resistance electrometer. The alternating polarity measurement method, which gives more repeatable conductivity measurement for high resistance materials, was used.[11]

The morphology of the composites was examined using a Philips XL30 scanning electron microscope. Composite sheets were cryogenically fractured and the fracture surfaces sputter coated with platinum.

Raman spectra were recorded at 2 cm^{-1} resolution using a Renishaw 1000 Raman imaging microscope consisting of a single-grating spectrograph, a Leitz microscope, and an air-cooled CCD array detector. The excitation laser had wavelength 785 nm.

An Instron 5567 universal testing machine was used to measure the mechanical properties of composite sheets in accordance with the ASTM D882-02 standard. The sample was about 15 mm wide and 0.3 mm thick. An Instron 2663-821 Advanced Video Extensometer with 200 field of view lens was used; the gauge length was about 50 mm. Two crosshead speeds were used, namely 5 mm min^{-1} for tensile modulus measurement and 50 mm $^{-1}$ for yield stress determination.

RESULTS AND DISCUSSION

X-ray diffraction

The powder X-ray diffraction patterns for polypyrrole [Fig. 1(a)] show a broad amorphous halo pattern with a distinct reflection centered at (2θ) about 25°, which is typical of the doped structure of polypyrrole.[12] The diffractogram for wollastonite [Fig. 1(b)] showed major reflections at about 11.5°, 23.2°, 25.3°, 26.9°, 38.3°, 41.3°, and 51.9°, which are in good agreement with reported data.[8] Except for the reflection at 29.4° and some small differences in the relative intensities of the reflections, the wollastonite reflections were detected in the coated filler [Fig. 1(c)]. The differences may indicate that the polypyrrole coating varied in thickness on the wollastonite crystal surfaces, as a result of variations in the surface energy of the crystal faces. The appearance of the wollastonite reflections at the same 2θ values after polypyrrole coating indicates that the coating did not affect the crystal structure of the substrate.

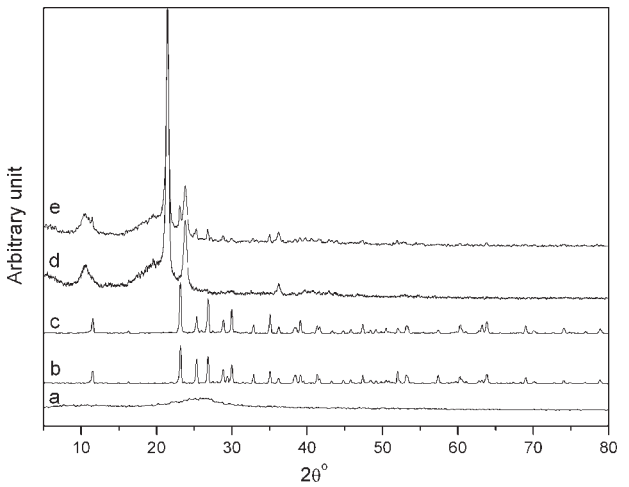

Figure 1 XRD diffractograms. (a) polypyrrole; (b) wollastonite; (c) wollastonite coated with polypyrrole; (d) polyethylene; (e) PE/EMA/wollastonite-ppy composite.

Figure 1(d,e) shows the diffraction patterns for the neat PE and the PE/EMA/wollastonite-ppy composite, respectively. The PE patterns show two principal crystalline reflections at 2θ values 21.4° and 23.7°, corresponding to the 110 and 200 lattice planes, respectively, and amorphous scattering centered at about 19.8°.[13] The broad reflection at about 10.4°, which was not reported by Qu and Ranby[13] is most likely also due to amorphous scattering. As shown in Figure 1(e), the composite has a diffraction pattern mainly from PE (because PE is the major component present) with some reflections of wollastonite, for example, at 11.5° and 23.2°. For simplicity, the diffraction pattern of EMA, which is similar to but less intense than that of PE, is not shown.

Thermal analysis

For polypyrrole [Fig. 2(f)], there was a weight loss of about 10% that is attributed to loss of residual water at temperatures up to about 100°C and pyrrole (with boiling point about 130°C). Degradation of polypyrrole in air began at about 260°C and at ~ 480°C, there is a small increase in the slope of the TGA curve, indicating that the rate of decomposition is more rapid above that temperature. It is apparent that polypyrrole is susceptible to oxidative decomposition in air with a greatly increased rate of decomposition at temperatures above about 260°C. The wollastonite and wollastonite-ppy samples had weight losses of about 3 and 15%, respectively, on heating to 800°C. The additional weight loss of about 12% from the coated filler can be partially attributed to the volatilization/decomposition of the polypyrrole coating, which should contribute about 5% (based on the 4.8% weight gain for wollastonite after coating with polypyrrole). The remainder of the weight loss cannot be easily accounted for and may be an instrumental artifact, because the recorded mass losses for samples d–f were somewhat greater than 100% at temperatures above about 700°C. It was observed, however, that the weight loss difference between wollastonite and polypyrrole-coated wollastonite was about 5% when heated in nitrogen (not shown). There is a small weight loss (2–3%) for wollastonite at about 700°C, which is close to the first-order phase transition temperature (995 K) that has a small enthalpy change (200 J mol^{-1}), reported for the common triclinic form of wollastonite by Richet and coworkers.[14] It is not observed for wollastonite-ppy, suggesting this transition was suppressed by the polypyrrole coating. The PE/EMA/wollastonite-ppy composite [Fig. 2(c)] had a degradation onset temperature of about 370°C, which was about 10 and 20°C higher than that of neat PE [Fig. 2(d)] and neat EMA [Fig. 2(e)], respectively. From the onset temperature to about 425°C, the weight loss of the neat PE and EMA was about 10% greater than that of the composite. This indicates the thermal stability of the composite compared to the neat PE and EMA in this temperature region. From about 425 to 480°C, the composite had slightly greater weight loss, which might be due to the decomposition of the polypyrrole and the EMA compatibilizer, and the TGA curve was very similar to that of neat EMA. Above 480°C, all the three TGA curves were almost identical.

Scanning electron microscopy and optical microscopy

Figure 3 shows a scanning electron micrograph of unmodified wollastonite particles. After sonication, individual particles with needle-like shape and

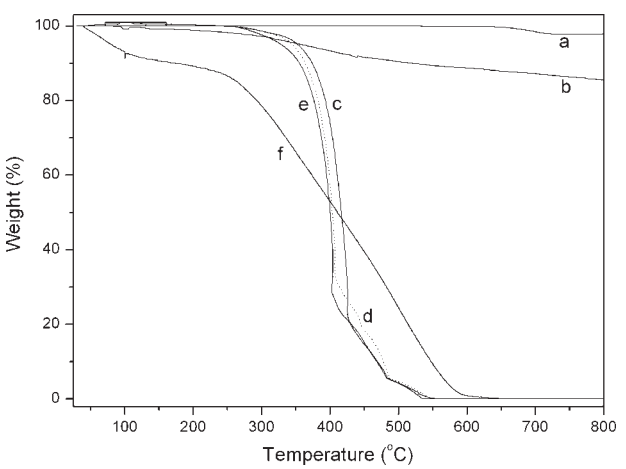

Figure 2 TGA scans of (a) wollastonite, (b) wollastonite-ppy, (c) PE/EMA/w-ppy composite, (d) polyethylene, (e) EMA, and (f) polypyrrole in air.

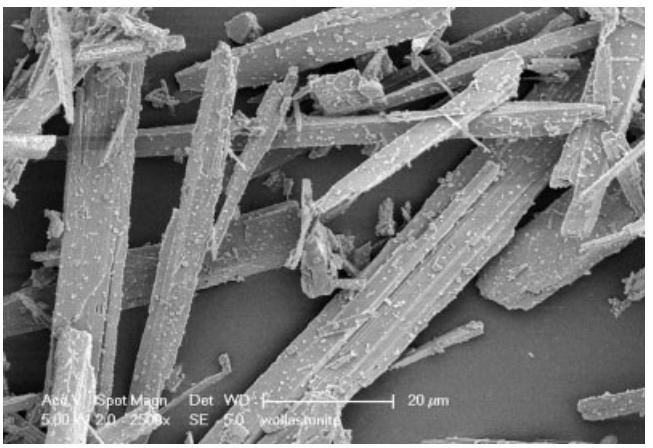

Figure 3 SEM micrograph of wollastonite particles.

aspect ratio typically of the order 10 (average length and width about 50 and 5 μm, respectively) were observed. A representative micrograph of polypyrrole-coated wollastonite is depicted in Figure 4, which clearly demonstrates the *in situ* growth of chemically synthesized polypyrrole in the form of nodules on the surfaces of wollastonite particles. It further indicates complete coverage of the surface of wollastonite with polypyrrole. Figure 5 presents an optical image of a thin film of PE containing this coated filler together with EMA as the compatibilizer. From this image, the presence of randomly dispersed fibrous wollastonite-ppy particles in the PE matrix is clearly evident. The SEM micrograph of a cryogenically fractured surface of the polypyrrole composites without any compatibilizer [Fig. 6(a)] shows a wollastonite-ppy particle partially embedded in the PE matrix with no discernible bonding between the matrix and the particle. By contrast, it is apparent from Figure 6(b,c) that the incorporation of EMA and MAPE caused much improved bonding

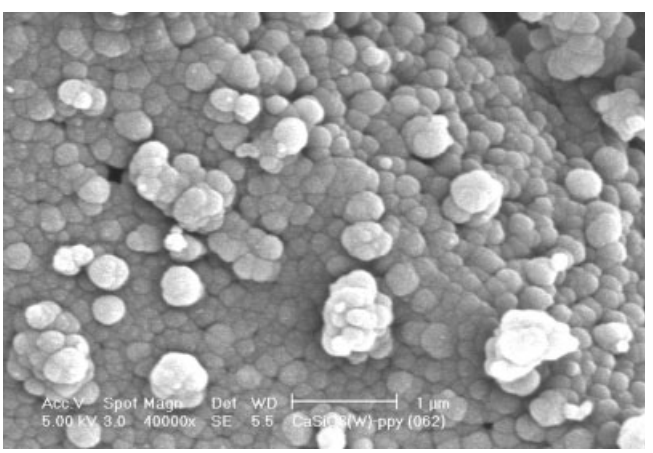

Figure 4 SEM micrograph of polypyrrole-coated wollastonite particle.

Figure 5 Optical micrograph of PE/EMA/wollastonite-ppy composite.

between PE matrix and wollastonite-ppy particles. The wollastonite-ppy particle in the center of the image in Figure 6(d) is surrounded by PE together with mostly spherical droplets of dispersed EVOH. The particle appears to be bonded to the matrix polymer, whereas Figure 6(e) shows less evidence of bonding between the wollastonite particle and the matrix. Figure 6(e) shows the additional feature that the dispersed compatibilizer appears to be partially fibrillized. It is significant that the surfaces of the wollastonite-ppy particles in Figure 6(d,e) are very much smoother than those in Figure 6(b,c), because the particles are covered with a coherent layer of EVOH or PVOH, due to the strong bonding interactions between ppy and materials containing highly polar functional groups such as OH.

Raman spectroscopy

Although PE can be melted and is stable during thermal processing, polypyrrole is infusible and susceptible to oxidation at high temperature, and it was important to ensure that polypyrrole was not decomposed in the extrusion process. Raman spectroscopy has been commonly used to study the structural stability of polypyrrole, and Figure 7 shows Raman spectra of (a) wollastonite, (b) polypyrrole, (c) wollastonite-ppy, (d) PE, (e) PE/EMA/wollastonite-ppy composite, and (f) EMA. The major bands of each spectrum are assigned in Table I. The wollastonite bands are attributed to the Si—O stretching above 800 cm^{-1}, Si—O bending between 500 and 760 cm^{-1}, and SiO_4 rotation and metal-oxygen translation below 500 cm^{-1}.[15] The polypyrrole spectrum [Fig. 7(b)] has the characteristic three double bands at about 930 and 981 cm^{-1} (ring deformation associated with bipolaron and polaron, respectively), 1047 and 1078 cm^{-1} (C—H in plane deformation), and 1328 and 1370 cm^{-1} (ring stretching mode of polypyrrole).[16,17] These bands are also observed in wollastonite-ppy [Fig. 7(c)] and PE/EMA/wollastonite-ppy [Fig. 7(e)] composites, which

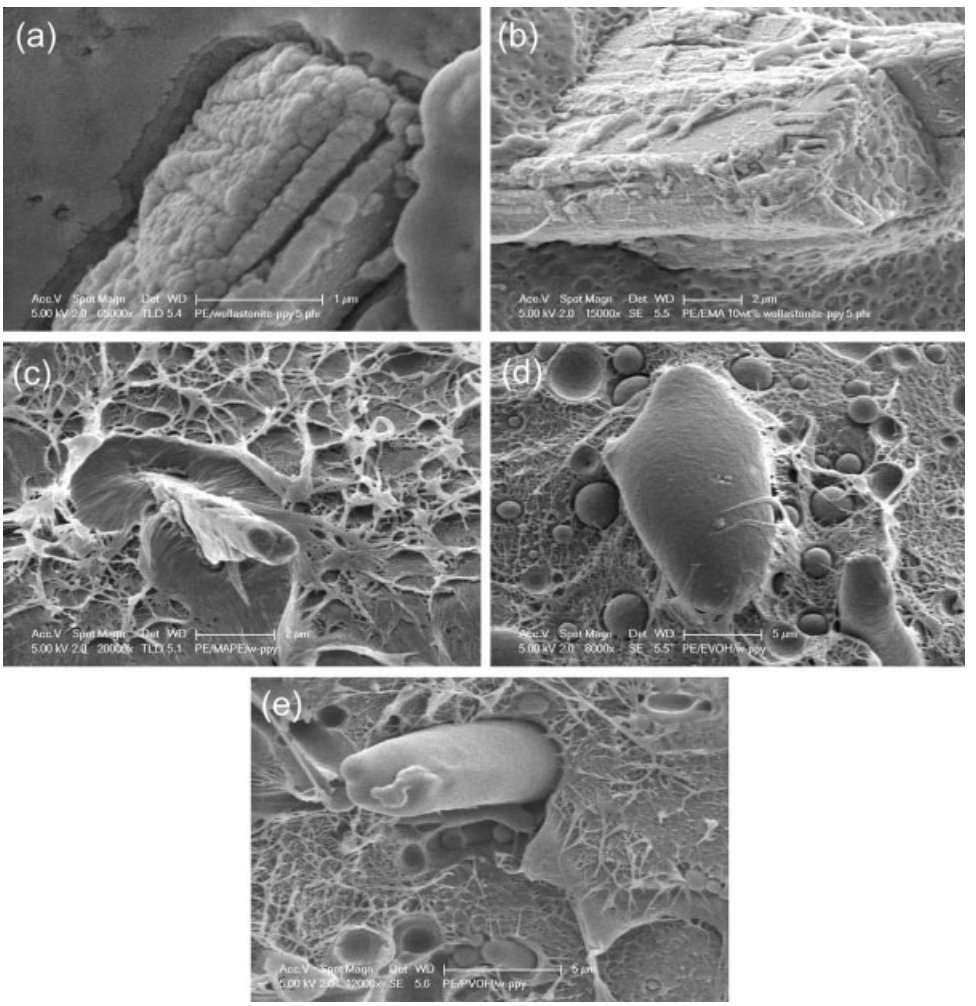

Figure 6 SEM micrographs of fractured surfaces of the composites: (a) PE/wollastonite-ppy; (b) PE/EMA/wollastonite-ppy; (c) PE/MAPE/wollastonite-ppy; (d) PE/EVOH/wollastonite-ppy; (e) PE/PVOH/wollastonite-ppy.

confirm the presence of polypyrrole in these materials. The spectra indicate that polypyrrole was not significantly oxidized with incorporation of oxygen during thermal processing at 180°C, because there was no C=O band at about 1740 cm^{-1}.[16] In addition, the υ(C=C) backbone stretch at about 1610 cm^{-1} for polypyrrole coated on wollastonite [Fig. 7(c)] and the PE composites [Fig. 7(e)] (i.e., both before and after extrusion) remained essentially unchanged, indicating the stability of the polypyrrole structure. The υ(C=C) backbone stretch for pure polypyrrole appears at about 1596 cm^{-1} [Fig. 7(b)], which is 14 cm^{-1} lower than that for wollastonite-ppy and the composite with PE. The difference in band positions is consistent with the pure polypyrrole being oxidized to a lesser extent than the polypyrrole coating on wollastonite, because the extent of oxidation of polypyrrole can be clearly related to the υ(C=C) backbone stretch band, which changes and shifts significantly compared to the other bands.[18] As the polypyrrole oxidizes certain sites of the polymer chain convert to the quinoid form (oxidized state) while some are still in the benzenoid form (reduced state), and both forms can coexist depending on the level of oxidation. For the extreme cases of polypyrrole electrochemically prepared by Santos and coworkers,[18] the υ(C=C) backbone stretch band appeared at about 1620 and 1557 cm^{-1} for the most oxidized state and most reduced state, respectively. The greater extent of oxidation of the polypyrrole coating is possibly attributable to the fact that it was formed as a coherent thin layer on the wollastonite surface rather than as a precipitate. In addition, the polypyrrole coating was formed in a more concentrated oxidant solution than was the case for the precipitated polypyrrole, although the mole ratio of oxidant to monomer was 2.4 in each case. In very recent work[19], we have found that if the same oxidant/pyrrole mole ratio and the same concentration of oxidant is used in both cases the υ(C=C) band shift is not observed (for polypyrrole coated on the silicate mineral halloysite).

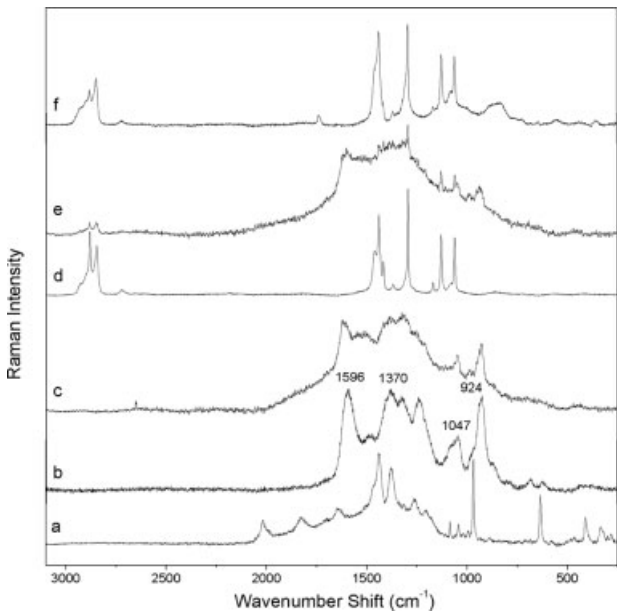

Figure 7 Raman spectra of (a) wollastonite, (b) polypyrrole, (c) wollastonite-ppy, (d) PE, (e) PE/EMA/wollastonite-ppy composite, and (f) EMA.

PE [Fig. 7(d)] has major bands at 1063, 1130, 1295, 1441, 2849, and 2883 cm^{-1}.[20] In addition to the bands from PE, EMA has a C=O band at about 1737 cm^{-1} [Fig. 7(f)]. Raman spectra confirm that polypyrrole was not degraded to a significant extent by the thermal processing of the composites. It is interesting to note that the wollastonite bands are not clearly seen for wollastonite-ppy most likely, because nearly all the red laser was adsorbed by the black conducting polymer coating, and there was minimal scattering from the wollastonite substrate.

FTIR

Figure 8 shows the IR spectra of the wollastonite, polypyrrole, wollasonite-ppy, and PE/EMA/wollastonite-ppy composite. The major bands of each spectrum are assigned in Table II. The polypyrrole spectrum shows the characteristic bands at 668, 789, 1315, 1456, and 1552 cm^{-1}.[6,21] The bands of wollastonite are generally attributed to Si—O—Si bending below 500 cm^{-1} and stretching at about 800–1200 cm^{-1}.[22,23] The spectrum of wollastonite-ppy [Fig. 8(c)] shows the characteristic bands of both wollastonite and polypyrrole. It is noted that the N—H stretching band frequencies for the polypyrrole and polypyrrole-coated wollastonite are different, which is most likely due to the interaction between the polyppyrrole and wollastonite. The spectrum of the composite [Fig. 8(d)] is dominated by the most intense bands at 2845 and 2915 cm^{-1} (C—H stretching and deformation vibrations) of PE,[24] because PE is the dominant component. For simplicity and because of their similarities, only the spectrum of the composite with EMA compatibilizer is shown here.

Mechanical properties of the composites

Figures 9 and 10 show the yield stress and tensile modulus of PE, PE/wollastonite-ppy, and the composites with the four compatibilizers. The modulus

TABLE I
Major Band Assignments for the Raman Spectra in Figure 7

Major bands (cm^{-1}) of Raman spectra						
EMA	PE/EMA/ w-ppy	PE	w-ppy	ppy	Wollastonite	Assignment
–	–	–	–	–	338, 411	Ca—O stretching
–	–	–	–	–	485	O—Si—O bending
–	–	–	–	–	636	Si—O—Si bending
–	930, 982	–	930, 982	930, 981	–	ring deformation associated with dication (bipolaron) and radical cation (polaron), respectively.
–	–	–	–	–	970	Si—O stretching
–	1047, 1077	–	1048, 1080	1047, 1078	–	C—H in plane deformation
1061	1061	1063	–	–	–	ν(C—C) stretching
1128	1129	1130	–	–	–	ν(C—C) stretching
1295	1296	1295	–	–	–	ν(C—C) stretching
–	1325, 1371	–	1325, 1370	1328, 1370	–	Ring-stretching mode of polypyrrole
1440	–	1441	–	–	–	$\delta(CH_2)$ and $\delta(CH_3)$ asymmetric
–	1610	–	1610	1596	–	ν(C=C) backbone stretching
1737	–	–	–	–	–	ν(C=O) stretching
2851	2851	2849	–	–	–	ν(CH) stretching
–	2885	2883	–	–	–	ν(CH) stretching

(a) Wollastonite, (b) polypyrrole, (c) wollastonite-ppy, (d) PE, (e) PE /wollastonite-ppy composite, and (f) EMA.

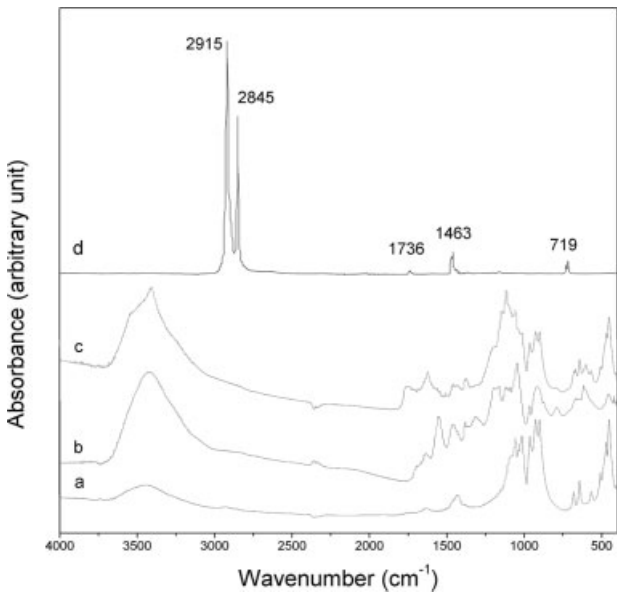

Figure 8 FTIR spectra of (a) wollastonite, (b) polypyrrole, (c) wollastonite-ppy, and (d) PE/EMA/wollastonite-ppy.

of neat PE was found to be about 637 MPa. Incorporation of 5 phr of polypyrrole-coated wollastonite in PE slightly increased the modulus to 690 MPa, whereas a decrease in modulus was observed in the case of PE/EMA/wollastonite-ppy (500 MPa) composite. The increase in modulus of PE/wollastonite-ppy composite could be due to the inherent modulus of wollastonite, because the incorporation of a stiffer material into a polymer matrix typically gives a composite with enhanced modulus. However, it is worthy to mention that the modulus of EMA was found to be only 20 MPa (using the same method that was used for the composites). As a result, in the case of PE/EMA/wollastonite-ppy composite, the increased modulus imparted to the composite by the wollastonite component is offset by the low modulus of the EMA. A similar argument applies to the PE/MAPE/wollastonite-ppy composite where the low modulus of MAPE (22 MPa) partially offsets the enhancement from the coated wollastonite particles. The substantially enhanced modulus (relative to PE) of the composite compatibilized with EVOH is consistent with the relatively large modulus (2745 MPa) of EVOH. The same argument almost certainly applies to the composite compatibilized by PVOH. PVOH-compatibilized film was found, qualitatively, to be very stiff, but its brittleness precluded reliable quantitative determination of tensile modulus.

The yield strengths of PE, PE/wollastonite-ppy, and the other composites were almost the same within experimental uncertainty (Fig. 10), which was contrary to our expectations based on the well-known ability of fibrous additives with moderately large aspect ratio and strong interphase bonding to reinforce thermoplastics such as PE and polypropylene. The aspect ratio of the wollastonite particles used in this work was thought to be sufficiently large to provide the enhancement of yield strength, but it is possible that the wollastonite particles were reduced in size by the high shear conditions in the screw extruder that was used to produce the composites, with consequential reduction in average aspect ratio of the particles. It is interesting to note that the composites made using the same processing method from PE with wollastonite coated with aminosilane, in which a strong bond was formed at the particle matrix interface, showed similarly no significant enhancement of tensile strength,[25] but a substantial increase in impact strength, relative to the matrix polymer.

TABLE II
Band Assignments for the FTIR Spectra in Figure 8

	Band assignment (cm^{-1}) of each spectrum[6,21–24]			
Wollastonite	ppy	w-ppy	PE/EMA/w-ppy	Assignment
400–500	–	400–500	–	δ(Si—O—Si) bending vibration
644, 681	–	644, 681	–	SiO_4 vibrations.
–	668, 789	670, 789	–	C—H outer bending vibrations
–	–	–	719	δ(CH_2) rocking deformation
800–1200	–	800–1200	–	ν(Si—O—Si) stretching modes of lattice vibrations
–	1315	–	–	=C—H in plane deformation
–	1456	1457	–	C—N stretching
–	–	–	1463	δ(CH_2) or δ(CH_3) asymmetric bending
–	1552	1554	–	pyrrole ring stretching
–	–	–	1736	ν(C=O) stretching of EMA
–	–	–	2845	ν(C—H_2) symmetric stretching
–	–	–	2915	ν(C—H_2) asymmetric stretching
–	3417	3407	–	ν(N—H) stretching
3447	–	–	–	ν(O—H) stretching

(a) Wollastonite, (b) polypyrrole, (c) wollastonite-ppy, and (d) PE/EMA/wollastonite-ppy.

Note the O—H stretch of wollastonite is attributed to trapped water molecules which were very difficult to remove. The band has been previously reported.[23]

Conductivity

The conductivities of the pristine polypyrrole powder and polypyrrole-coated wollastonite were 0.1 S cm^{-1} and about 1.2×10^{-6} S cm^{-1} at ambient temperature, respectively. This difference in conductivity can be attributed to the relatively small proportion ($\sim$ 4.8 wt %) of polypyrrole in the polypyrrole-coated wollastonite. The polypyrrole content and the conductivity were comparable with those reported by Micusik et al.,[7] namely a conductivity range from about 10^{-7} to 10^{-3} S cm^{-1} for polypyrrole contents in the range 2.5–7 wt %. After being incorporated into PE at 5 phr loading, the conductivity of the composite (containing about 0.25% polypyrrole) was about one to two orders of magnitude higher than for the PE (4×10^{-14} S cm^{-1}). The conductivity values for PE/wollastonite-ppy, PE/EMA/wollastonite-ppy, PE/MAPE/wollastonite-ppy, PE/EVOH/wollastonite-ppy, and PE/PVOH/wollastonite-ppy were 1×10^{-13}, 1.5×10^{-13}, 8×10^{-14}, 2×10^{-12}, and 2.3×10^{-12} S cm^{-1}, respectively. The low conductivity of the composites was not unexpected in view of the very small amount of conducting polypyrrole present. It is interesting, however, that the conductivities of the EVOH and PVOH-compatibilized composites were about two orders of magnitude higher than that of PE itself despite the coated filler particles being covered (as indicated by the SEM micrographs) with a relatively thick layer of compatibilizer. This could possibly be explained by the availability of some particles in very close proximity providing a route with less resistance in the composite film. For comparison, one type of the composites was loaded with more wollastonite-ppy (up to 20 phr), and the conductivities increased slightly as the loading increased, which gave 2×10^{-13}, 2.4×10^{-13}, and 2.8×10^{-13} S cm^{-1} for 10, 15, and 20 phr, respectively. The conductivities are still very low, however, most likely due to the lack of an established conducting network in the composites, and thus the percolation threshold was not reached.

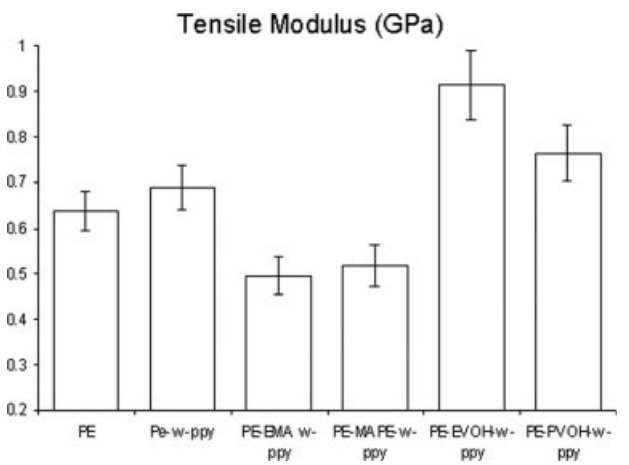

Figure 9 The tensile modulus of PE and the composite materials.

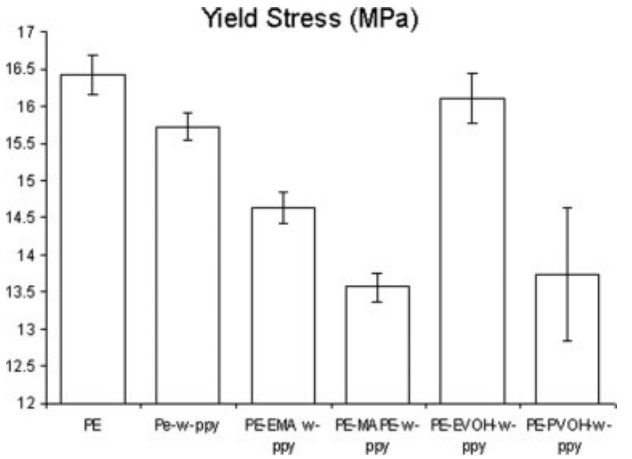

Figure 10 The yield stress of PE and the composite materials.

CONCLUSIONS

Wollastonite particles precoated with polypyrrole can be incorporated into PE using a single screw extruder, and the resulting composites can be formed into sheets by compression molding. The weak interaction between the coated filler particles and the matrix polymer is substantially enhanced by EMA, MAPE, EVOH, and to a lesser extent by PVOH, used as compatibilizers. In composites containing EVOH or PVOH, polypyrrole-coated wollastonite particles become coated with compatibilizer, due to strong interaction between polypyrrole and OH groups in those compatibilizers. Despite the strong particle-matrix interactions in composites compatibilized with EMA, MAPE, and EVOH, the yield stresses of these composites are not significantly enhanced relative to the PE matrix polymer. However, the tensile moduli of the composites compatibilized with EVOH and PVOH are more than 20% greater than that of the matrix polymer.

References

1. Zhang, Q.; Wang, X.; Chen, D.; Jing, X. J Polym Sci Part B: Polym Phys 2004, 42, 3750.
2. Paul, R. K.; Pillai, C. K. S. J Appl Polym Sci 2002, 84, 1438.
3. Yang, J. P.; Rannou, P.; Planes, J.; Pron, A.; Nechtschein, M. Synth Met 1998, 93, 169.
4. Xue, P.; Tao, X. M. J Appl Polym Sci 2005, 98, 1844.
5. Poopathy, K.; Adams, P. N.; Marsh, A. M.; Shah, D. Eur. Pat. 298,746 (1989).
6. Cheng, Q.; Pavlinek, V.; Lengalova, A.; Li, C.; He, Y.; Saha, P. Micropor Mesopor Mater 2006, 93, 263.
7. Micusik, M.; Omastova, M.; Nogellova, Z.; Fedorko, P.; Olejnikova, K.; Trchova, M.; Chodak, I. Eur Polym J 2006, 42, 2379.
8. Liu, X.; Ding, C.; Wang, Z. Biomaterials 2007 2001, 22.

9. Yuan, X. W.; Easteal, A. J.; Bhattacharyya, D. Proceedings of the 28th Australasian Polymer Symposium and the Australasian Society for Biomaterials 16th Annual Conference, Rotorua, New Zealand, Feb 5–9, 2006.
10. Li, X.; Chang, J. Chem Lett 2004, 33, 1458.
11. Model 6517A Electrometer User's Manual; Keithley Instruments, Inc, USA, 2003, pp 2–63.
12. Allen, N. S.; Murray K. S.; Fleming, R. J.; Saunders, B. R. Synth Met 1997, 87, 237.
13. Qu, B. J.; Ranby, B. J Appl Polym Sci 1993, 48, 711.
14. Richet, P.; Robie, R. A.; Hemingway, B. S. Eur J Miner 1991, 3, 475.
15. Huang, E.; Chen, C. H.; Huang, T.; Lin, E. H.; Xu, J. A. Am Mineralogist 2000, 85, 473.
16. Han, G.; Yuan, J.; Shi, G.; Wei, F. Thin Solid Films 2005, 474, 64.
17. Kilmartin, P. A.; Li, K. C.; Bowmaker, G. A.; Vigar, N. A.; Cooney, R. P.; Travas-Sejdic, J. Curr Appl Phys 2006, 6, 567.
18. Santos, M. J. L.; Brolo, A. G.; Girotto, E. M. Electrochim Acta 2007, 52, 6141.
19. Ong, C. K.; Ray, S.; Edmonds, N. R.; Easteal, A. J. J Appl Polym Sci, to appear.
20. Raman, R. K. S.; Fekitoa, P.; Bandyopadhyay, S. J Mater Sci Lett 1998, 17, 289.
21. Kurachi, K.; Kise, H. Polym J 1994, 26, 1325.
22. Chen, S. K.; Liu, H. S. J Mater Sci 1994, 29, 2921.
23. Zhao, J.; Wang, Z.; Wang, L.; Yang, H.; Zhao M. Mater Lett 1998, 37, 149.
24. Bajer, K.; Kaczmarek, H.; Dzwonkowski, J.; Stasiek, A.; Oldak, D. J Appl Polym Sci 2007, 103, 2197.
25. Yuan, X. W.; Bhattacharyya, D.; Easteal, A. Key Eng Mater 2007, 334–335, 265.